Mol Biotechnol (2009) 41:69–82
DOI 10.1007/s12033-008-9107-y

REVIEW

Nanosecond Electroporation: Another Look

Raji Sundararajan

Published online: 26 September 2008

Abstract As the medical field moves from treatment of diseases with drugs to treatment with genes, safe and efficient gene delivery systems are needed to make this transition. One such safe, non-viral, and efficient gene delivery system is electroporation (electrogenetherapy). Exciting discoveries using electroporation could make this technique applicable to drug and vaccine delivery in addition to gene delivery. Typically milli and microsecond pulses have been used for electroporation. Recently, the use of nanosecond electrical pulses (10–300 ns) at very high magnitudes (10–300 kV/cm) has been studied for direct DNA transfer to the nucleus in vitro. This article reviews the work done using high-intensity nanosecond pulses, termed as nanosecond electroporation (nsEP), in electroporation gene delivery systems.

Keywords Nanosecond pulses · Electroporation · Membrane breakdown · Calcium burst · Apoptosis · Caspase

Introduction

Many potential drugs that have been developed to treat cancer and other diseases have found limited success due to the lack of efficient and safe delivery systems that allow the molecules to cross the cell plasma membranes. Due to the difficulty in passing though both the hydrophilic and hydrophobic portions of the lipid bilayer, the membranes are impermeable to these molecules. Electroporation or electropermeabilization (EP) is a technique that utilizes precisely controlled electric fields of short duration and high intensities to open up transient pores (aqueous pathways) through semi-permeable membranes and tissues allowing targeted delivery of therapeutic materials including drugs, antibodies, and genes (DNA) [1–3]. EP has been shown to offer a 100–1000-fold improved therapeutic benefit compared to using a drug alone, and is gaining acceptance as a viable technique to enhance the efficacy of drug delivery for cancer treatment, gene transfer, and similar applications in biology, biotechnology, and medicine [4–6]. Electroporation-mediated chemotherapy—Electrochemotherapy (ECT) is a viable alternative to conventional cancer treatments as evidenced by successful Phase I and II clinical trials for various skin cancers, such as lymphomas, squamous cell carcinomas, testicular carcinomas, and malignant pleural effusions [1, 5, 6]. There are isolated reports of cases of vocal chord and oral cancer, pancreatic cancer, brain tumors, and hepatic metastases that have been successfully treated using this technique. For cases, when surgery, radiotherapy, and/or chemotherapy failed, EP was found to be effective for the treatment of breast cancer [7].

EP is a physical phenomenon resulting from the interaction of the plasma membrane with the electric field, and it can be applied to all histological types of solid tumors. EP increases the permeability of the cell membranes by dielectric breakdown allowing temporary access to the cell interior (reversible electroporation). The cell membrane is then resealed once the application of pulses is stopped. It is generally accepted that membrane breakdown occurs if the induced membrane voltage reaches a value of about 1 V at room temperature. EP has gained common acceptance in many areas of biotechnology and medicine because it is

R. Sundararajan (✉)
ECET Department, Purdue University, W. Lafayette, IN 47907, USA
e-mail: rajis@ieee.org

more controllable, reproducible, and efficient than alternative chemical and viral techniques.

Typically, 1300 V/cm, 100 μs pulses were used for skin cancer trials [1, 5]. Most studies have used six or eight pulses with an interval of 1 s (1 Hz) [1, 2, 5]. For gene therapy, lower intensity and longer pulses, such as 125 V/cm, 25 ms [8]; 200 V/cm, 10 ms [9] have been found to be effective. Lately, ultra-short pulses of nanosecond (ns) durations and 10–300 kV/cm (nsEP) have been used for electroporation [10–14]. Under these conditions, the plasma membrane acts as a short circuit allowing the pulse to directly manipulate the internal organelles of the cell [15]. Hallmarks of apoptosis, including phosphatidylserine (PS) translocation, and caspase activation have been observed with high-intensity nanopulse electroporation. With these effects, it is expected that the use of ultra-short pulses of sub-microsecond or nanosecond durations could be used for additional applications in biotechnology and medicine, specifically for cancer/gene therapy. The use of high-intensity DC pulses with durations shorter than the time constant of membrane charging (1 μs) can offer valuable insight into the biophysical mechanisms involved in the electropermeabilization of the cells [10–12]. However, due to the complexity of the design and the high cost involved in constructing a nanoelectroporation system, there is no commercially available nanopulsers. Technical advancements in the field of pulsed power equipment [16, 17] have enabled a few researchers to conduct nsEP studies, in which the efficiency of ultra-short electric pulses for the reversible permeabilization of mammalian cells has been explored. To this end, nanopulse generators, delivering unipolar square pulses with electric field strengths up to 300 kV/cm and as small as 10 ns, were built and tested. Various cells, such as human Jurkat T lymphoblasts, HL-60, and mouse myeloma cells were studied using these pulsers.

Frequency Response of Cells

Charges accumulate at the plasma membrane of a biological cell when a voltage pulse is applied, and the induced potential across the membrane is increased [15, 18, 19]. Depending upon the magnitude, duration, and the frequency of the voltage applied, the cell membranes can temporarily break down, creating pores that can eventually be resealed. The membrane potential V_m is given as [15]:

$$V_m = 1.5 \times E \times R \times \cos(\delta)/[1 + R \times G_m(\rho i + 0.5 \times \rho a) \times (1/(1 + j\omega T))] \quad (1)$$

where ρi and ρa are resistivities inside and outside the cell, respectively, R is the cell radius, δ is the angle between the electric field E and the radius vector, ω is the radian frequency $= 2\pi f$, where f is the frequency, T is the time constant, and G_m is the membrane conductance. Assuming that the cytoplasm and the external medium are purely resistive, the influence of their dielectric constants can be neglected. If the conductance is also neglected, the membrane potential is given as:

$$V_m = 1.5 \times E \times R \times \cos(\delta)/(1 + j\omega T);\ \text{magnitude},$$
$$V_m = 1.5 \times E \times R \times \cos(\delta)/\sqrt{(1 + \omega T)^2} \quad (2)$$

Equation 2 can be considered as the general expression for the induced plasma membrane potential at all frequencies. When $\omega T \ll 1$ or $f = 0$, as in the dc case, Eq. 2 becomes the well-known frequency-independent expression:

$$V_m = 1.5 \times E \times R \times \cos(\delta) \quad (3)$$

At very low frequencies, the internal field strength is zero, if the membrane conductance is neglected, and the cell interior is shielded by the capacitive membrane. Thus, the membrane receives the total potential applied to the cell, thereby enhancing the external field strength to the membrane field strength level by several fold. On the other hand, at very high frequencies, the membrane capacitance is short-circuited and the total potential applied to the cell by the external field is available to the cytoplasm [15] and the internal organelles. Thus, the nsEP effect can "reach inside" cells, disrupting internal membranes causing calcium release, apoptosis, and other events normally associated with internal cell-biological signaling [11].

A simulation study of the behavior of cells at various frequencies correlates very well with the above concept [20]. At low frequencies, the outer plasma membrane with large capacitance is affected, and at high frequencies, the outer membrane is shorted and the applied voltage appears mainly across the interior of the cell. Thus, at low frequencies, the potential across the interior is very small. As the frequency increases, the input voltage is applied across the internal organelles of the cell. Figure 1 illustrates this concept. This also correlates very well with the recent nanosecond pulse results of Beebe et al. [11]. Using 10–300 ns pulses and tens of kV/cm fields, they observed that as the pulse durations decrease, the effect on the external plasma membrane decreases and effects on intracellular signal transduction mechanisms increase. Thus, the interaction of electric fields and biological cells also depends upon the frequency of the voltage applied. This is due to the frequency dependency (dielectric dispersion) of the relative permittivity (dielectric constant) and conductivity

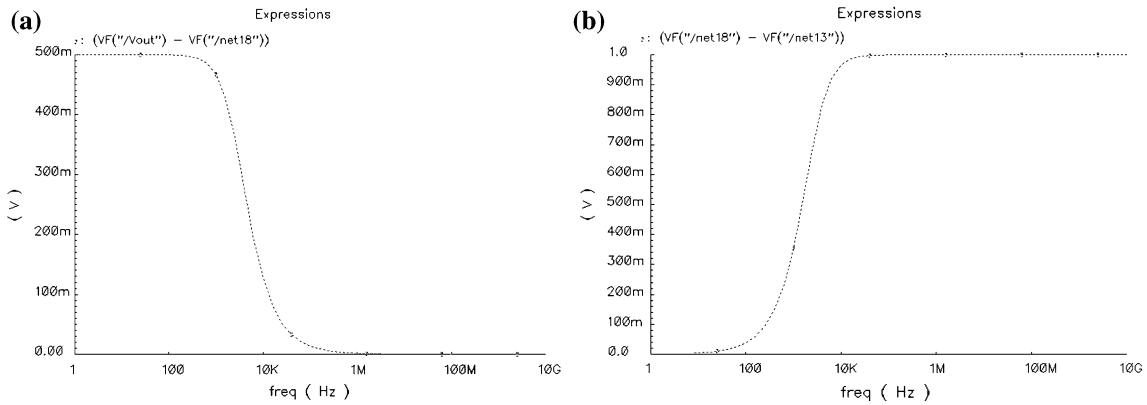

Fig. 1 Frequency response across the outer cell membrane (**a**) and across the interior of the cell (**b**). At low frequencies, the outer plasma membrane has more induced voltage. At high-frequency electric field, the outer membrane is shorted and the input voltage is applied across the inner membrane. At low frequencies there is no voltage across the nucleus. As the frequency is increased to megahertz range or nanosecond pulse range, we can gain control over the nucleus [20]

(or resistivity) of the tissues over the total frequency range, from a few Hz to several GHz [21].

Nanoelectroporation

High-frequency nanosecond pulses of high intensity can "reach inside" cells, disrupting internal membranes causing calcium release, apoptosis, and other events normally associated with internal cell-biological signaling [10, 11]. When applied in physiological media, they can produce significant voltages across intracellular membranes, such as the nucleus, mitochondria, storage vacuoles, Golgi compartments, and the endoplasmic reticulum, without irreversibly porating the plasma membrane. The primary effect of nanopulses is the perturbation of internal organelles with little or no effect to the plasma membrane (Fig. 2) [22]. The induction of apoptosis, including PS externalization, calcium bursts, caspase activation, etc. can be considered as secondary effects. Thus, ns pulses can physically manipulate intracellular structures in a precise manner with a wide range of amplitudes, durations, and patterns, extending the reach of the electric field past the cytoplasmic membrane to the internal membranes of the cell. Even when the plasma membrane is reversibly permeabilized, the extent of permeation and the resultant physiological and morphological changes are different from those seen with conventional electroporation [11, 22].

While nsEP has its own specific characteristics, like classical electroporation, its effects also depend on the magnitude, duration and number of pulses, type of cell, the conductivity of the medium, etc. as observed from the noticeable differences in the responses of the Jurkat cells and the mouse myeloma cells [13].

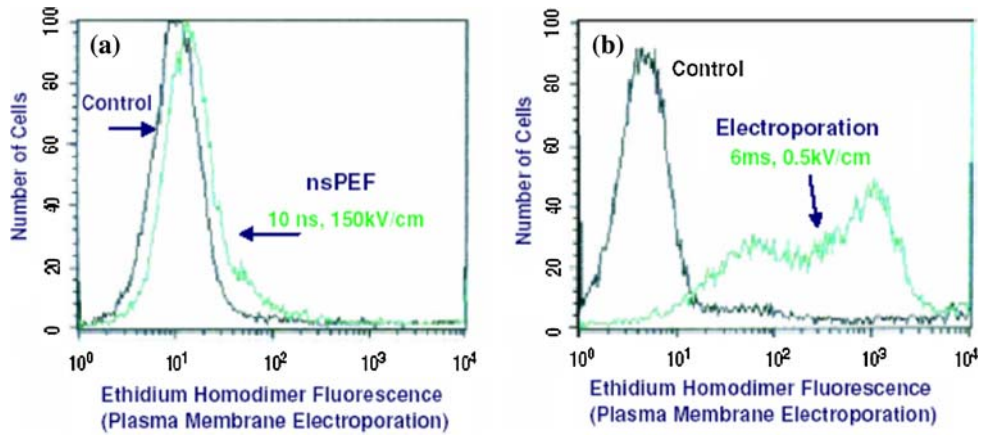

Fig. 2 Comparison of nsEP and classical plasma membrane electroporation in human Jurkat cells [22]. Cells were exposed to a single 10 ns pulse at 150 kV/cm and a single 6 ms pulse at 500 V/cm in the presence of ethidium homodimer-1 and were analyzed by flow cytometry. As expected, the 10 ns pulse did not have any significance on the plasma membrane, while the 6 ms pulse at an energy density of only 50% of that of the 10 ns pulse resulted in considerable increase in ethidium homodimer-1 fluorescence, indicating significant disruption of the plasma membrane

nsEP Effects

Apoptosis

Apoptosis, also known as programmed cell death or the selective suicide of cells, can be induced in a number of ways, such as nutrient exhaustion, growth factor deprivation, toxin accumulation [23], cross-linking of the CD95 molecule, ionizing radiation, glucocorticoids, cytotoxic T cell activity, long duration current, serum removal, and a variety of other means [24–26]. Apoptosis is characterized by specific morphological and biochemical alterations of the cell including membrane blebbing, chromatin condensation, DNA fragmentation, and the degradation of intracellular proteins such as poly(ADP-ribose) polymerase (PARP), lamin, and others [24–27]. Apoptosis is also induced by electric pulses of both classical electroporation and nsEP [10, 13, 14, 22, 24]. Induction of apoptosis was reported by Zimmermann's group where Jurkat cells suspended in R-10 culture medium were subjected to a single, exponentially decaying electrical pulse of 40 μs duration and of intensities from 3.6 to 8.1 kV/cm. Treatment of cells with pulses above 4.5 kV/cm readily induced DNA fragmentation [24]. The degree of fragmentation increased with an increase in field intensity. Similar nanopulse-induced DNA fragmentation was also observed in HL-60 cells in a voltage-dependent fashion [10, 22].

Apoptosis in human Jurkat and HL-60 cells were observed by Schoenbach's group with the application of pulses of 10–300 ns, and up to 300 kV/cm [11, 22, 28]. Flow cytometry was used to characterize apoptosis induction using annexin V binding and caspase activation. Table 1 shows the details of apoptosis experienced in a study where Jurkat cells were exposed to three 60 ns, 60 kV/cm pulses at 1 s interval [11]. Flow cytometry with ethidium homodimer and Annexin-V-FITC were used for the analysis. The markers were added 5, 10, and 30 min after pulsing. Before pulsing, 89% of the cells were normal and non-apoptotic as evidenced by their intact plasma membrane (no ethidium fluorescence), and there was no phosphatidylserine on the outer cell membrane as evidenced by the absence of Annexin-V-FITC fluorescence. Five minutes after pulsing, 80% of the cells were apoptotic as evidenced by intact cell membrane (no ethidium fluorescence) and translocation of phosphatidylserine to the outer cell membrane as evidenced by Annexin-V-FITC fluorescence. The apoptosis decreased at longer durations of 10 and 30 min. However, the decrease in apoptosis was accompanied by an increase in necrosis in these durations. Similar results were also obtained for other nanopulses of 300 ns, 26 kV/cm and 10 ns, 150 kV/cm strengths. Compared to 60 ns pulses, the apoptotic markers were more intense in the case of 300 ns pulses, and were less intense for the 10 ns pulses. These results illustrate that nsEP affects the cell interior and activates signaling pathways for apoptosis induction. Figure 3 illustrates apoptosis as reported by Schoenbach et al. [28].

Table 1 Nanopulse-induced apoptosis in Jurkat cells—three 60 ns, 60 kV/cm pulses 1–2 s intervals—analysis by flow cytometry [11]

Item	% Live cells	% Apoptotic cells	% Necrotic
Control	84.5 ± 1.9	12.3 ± 2.5	1.8 ± 0.5
Pulsed-after 5 min	4.2 ± 0.7	82.2 ± 1.3	12.8 ± 1.4
Pulsed-after 30 min	2.1 ± 0.9	70.0 ± 2.8	26.8 ± 3.7

Apoptosis was also observed by Vernier et al. [13, 14] in their studies using Jurkat cells with 10 ns and 20 to 40 kV/cm pulses. In their studies [13], they observed different sensitivities to the two cell types they used, the human Jurkat cells and the mouse myeloma cells, affirming the fact that electroporation (conventional or nano) parameters vary from cell to cell and each cell needs to be optimized for its applications.

Phospholipid Phosphatidylserine externalization

A common feature of the apoptotic process is the induced translocation of the phospholipid phosphatidylserine to the

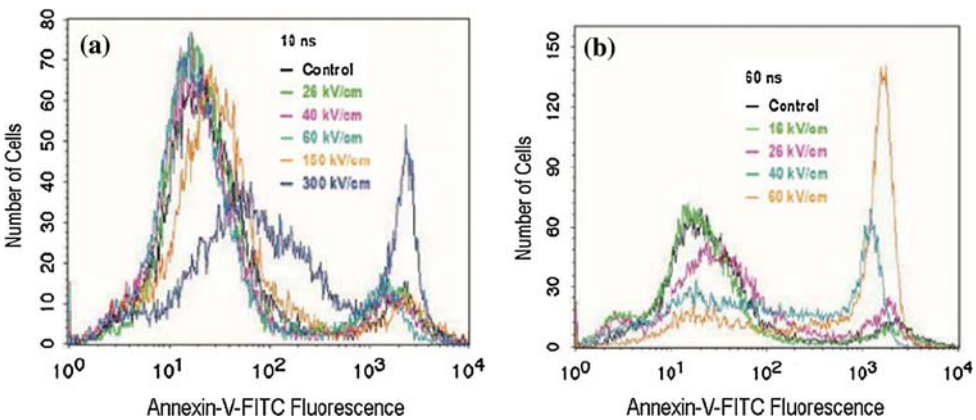

Fig. 3 Nanosecond pulse-induced apoptosis in Jurkat cells [28]. The cells were subjected to 10 ns, and up to 300 kV/cm (**a**) and 60 ns, and up to 60 kV/cm (**b**) pulses and were analyzed for Annexin-V-FITC fluorescence using flow cytometry. In both cases, the apoptosis increased with increased electric field strength. Increased Annexin-V-FITC fluorescence also indicates PS externalization

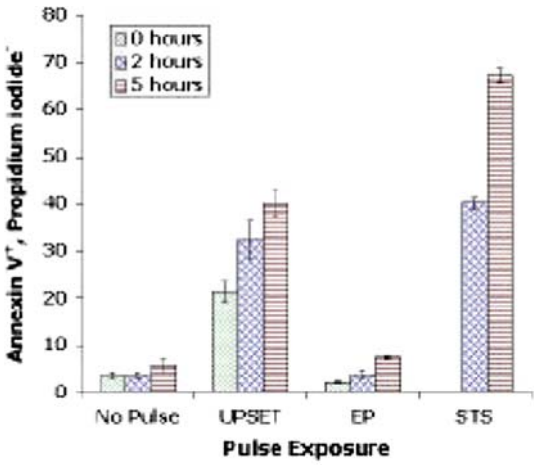

Fig. 4 Comparison of PS externalization at nano and classical electroporation conditions using annexin V binding at various durations—0, 2, and 5 h. Pulses applied were: 50 pulses of 10 ns, 25 kV/m (UPSET) and classical electroporation (one pulse at 500 μs and 600 V/cm [13]). Staurosporine (STS), a protein kinase C inhibitor and apoptosis-inducing agent, serves as a positive control

outer leaflet of the plasma membrane [25]. PS-dependent signaling is coupled to the final common pathway of apoptosis, i.e., the caspase-driven dismantling of the cell, thus allowing for effective phagocytosis and clearance of all corpses [29]. In cellular plasma membranes, PS is normally located on the internal leaflet of the lipid bilayer. The internal PS is externalized when the cells undergo apoptosis [30]. Thus, apoptosis is associated with the externalization of PS in the plasma membrane and subsequent recognition of PS by specific macrophage vectors [29].

Induction of PS externalization by nsEP was reported by Vernier et al. [13, 31]. More than 30% of cells showed evidence of PS externalization when assayed immediately after exposure to fifty 7 ns, 25 kV/cm pulses at 20 Hz. This was studied using annexin V-FITC, the fluorescent-marker with high affinity for PS. This indicates the translocation of PS to the external leaflet of the membrane lipid bilayer due to the high-intensity nanopulses. Fewer than 5% of control cells (no pulse exposure) showed annexin V-FITC binding. Flow cytometry of the cells subjected to ns pulses indicated that exposure of mammalian cells to ns, high-intensity electric pulses produced a rapid, dose-dependent translocation of PS to the external face of the cytoplasmic membrane (Fig. 4) [13]. Recent experiments with HCT116 colon carcinoma cells have shown that the translocation of PS can, when induced by nanosecond pulses, be reversible [32].

Caspases

Caspases are a group of cysteine proteases that play a crucial role in apoptotic pathways induced by a variety of stimuli. These enzymes act as important messengers and lead to the disassembly of the cell. Caspases are activated either by a ligand binding of a death receptor that leads to rapid induction of initiator caspases or by mild cytotoxic stimuli, which simulates the release of cytochrome c and apoptosis inducing factor from mitochondria in a protracted manner. Activated caspases cleave a variety of intracellular proteins including major structural elements, a number of protein kinases and the DNA repair machinery, and thus disrupting cell survival pathways. Deregulation of apoptotic pathways and of caspase activity contributes to a large number of pathological conditions, including neurodegenerative disorders, auto-immune disease, and cancer. Hence, caspases have become the primary targets for therapeutic interventions in these diseases.

Nanosecond electric fields can induce caspase activation along with other intracellular effects as reported by Beebe et al. and Vernier et al. [11, 13, 33]. Human Jurkat cells were pulsed with 5 ns pulses at 1 s intervals with various intensities and durations (Fig. 5), and were analyzed by flow cytometry after 20 min incubation with the cell permeable, irreversible, fluorescent inhibitor of active caspases, VAD-fmk-FITC. Figure 5 shows the presence of active caspases in intact cells [33]. The longer the pulses, the greater the observed caspase activity [13, 33]. Caspase active cells were reduced in size and had intact membranes.

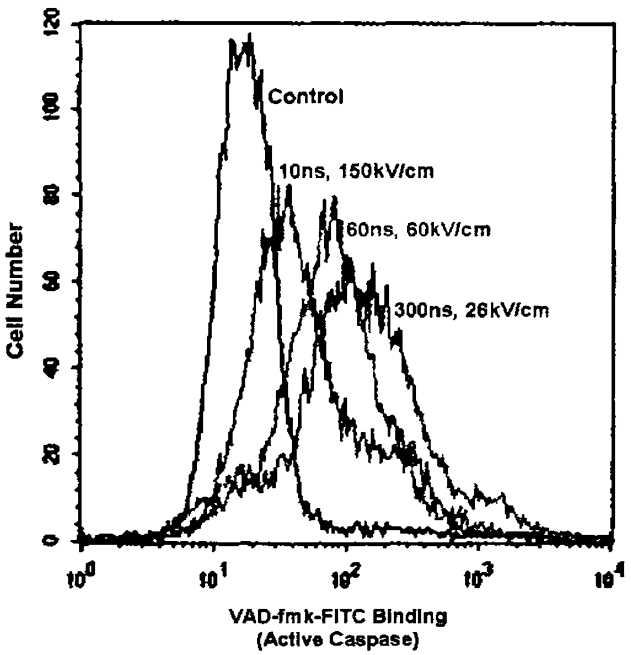

Fig. 5 Caspase activation in Jurkat cells due to nsEP [33]. The VAD-fmk-FITC binding indicates active caspase in intact cells

Calcium Bursts

The initiation of calcium bursts due to nsEP has also been reported by various researchers [14, 28]. Human Jurkat T lymphoblast cells loaded with a calcium-sensitive fluorochrome, calcium green, and suspended in RPMI growth medium containing 5 μg/ml propidium iodide showed no morphological signs of electroporation when exposed to 10 30 ns, 25 kV/cm pulses [14]. However, a marked intensification of calcium green fluorescence was seen within seconds of pulse exposure, indicating an increase in the intracellular calcium ion concentration ($[Ca^{2+}]i$). The calcium green fluorescence intensification was uniform across the cell. No single or multiple release points were noticed. The calcium green fluorescence increased everywhere inside the cell at once, within the limits of the resolution of these observations (approximately 100 ms and 0.4 μm). It is presumed that this phenomenon must have originated from the cell and was not due to the propagation of a calcium wave from a disturbance in the plasma membrane. Figure 6 illustrates the calcium burst experienced in this research [14]. A detailed study of the source of calcium burst speculates that the nanopulses at high intensity could have stimulated the release of calcium from ER compartments.

Experiments with Jurkat cells loaded with calcium green marker showed that calcium release is coupled to PS externalization [28]. The pulses applied to the cells were 30 ns long at an amplitude of 25 kV/cm. Although PS externalization is an apoptosis marker, it does not necessarily lead to cell death. Additional results were obtained by Beebe et al. [22]. In this study, nanopulsed HL-60 cells released significant amount of intracellular calcium with 8–10-fold increase in magnitude, after exposure to a single 60 ns, 15 kV/cm pulse. This was identified using UTP. The threshold for the release of Ca^{2+} was found to be field intensity dependent. There was a 4-fold increase with 4 kV/cm nanopulse, and a 15-fold increase with a 15 kV/cm pulse, compared to base level in the presence of extracellular Ca^{2+}. Again, it was speculated that nsEP induced calcium mobilization from intracellular reserves, followed by possibly capacitive induced increases in calcium from the extracellular environment through the plasma membrane.

Cytochrome C Release

To verify if the nanopulse-induced apoptosis is based on a mitochondrial-dependent mechanism, the presence of cytochrome c in the cytoplasm was studied by Beebe et al. [11]. Here, Jurkat cells were exposed to three nanosecond pulses at 1 s interval. The various pulses applied were: 10 ns, 150 kV/cm; 60 ns, 60 kV/cm; and 300 ns, 26 kV/cm. The energy density was approximately the same (1.7 J/cc/pulse) in all these cases. Cell extracts were separated into cytosol and mitochondrial fractions and analyzed for cytochrome c by immunoblot analysis. The results indicated the presence of cytochrome c in the nanopulsed cells (Fig. 7) [11]. Cytochrome c release from the mitochondria into the cytoplasm suggests that the apoptosis induced by the nsEP is indeed dependent on mitochondria. However, it is not clear if mitochondria are primary or secondary

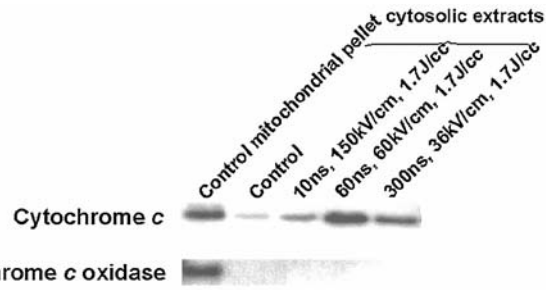

Fig. 7 Immunoblot analysis of Jurkat cells for cytochrome C release into the cytoplasm due to nsEP-cells were exposed to three 10 ns, 150 kV/cm; 60 ns, 60 kV/cm; and 300 ns, 36 kV/cm pulses at 1 s intervals [11]

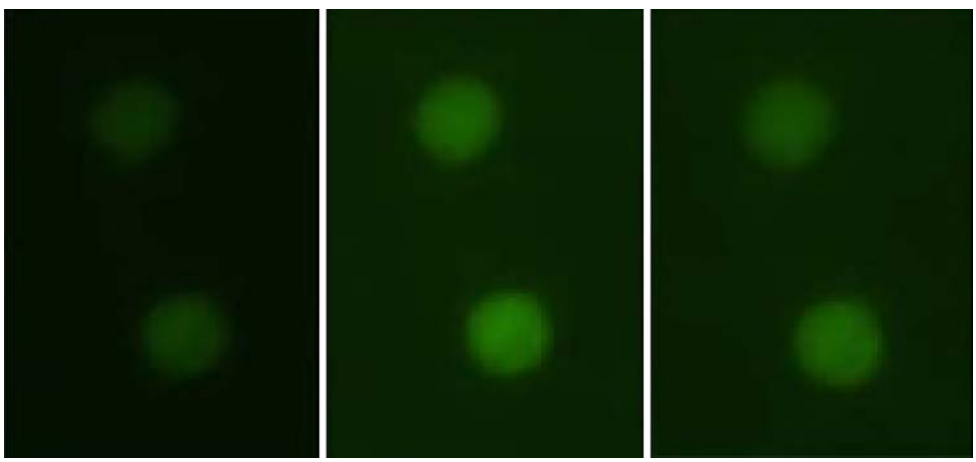

Fig. 6 Real time intracellular calcium release due to nsEP. Jurkat cells were exposed to 10 30 ns, 25 kV/cm pulses. These pulses did not uptake propidium iodide (marker for plasma membrane disintegrity) but caused intensification of the fluorescence of the calcium-sensitive fluorochrome calcium green marker, indicating an increase in the intracellular calcium ion concentration [14]

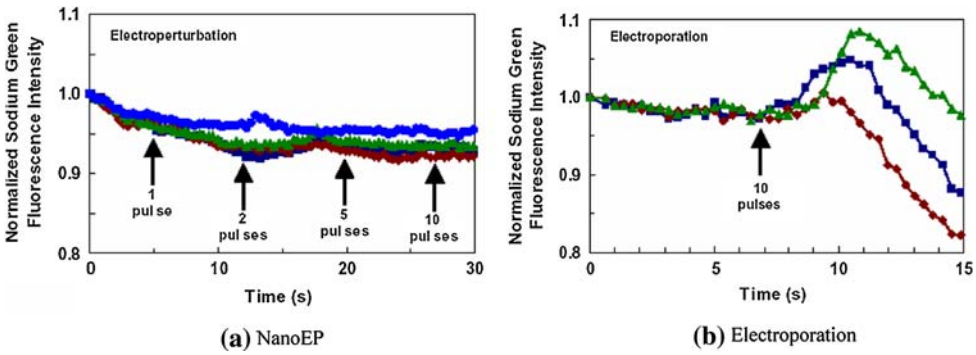

Fig. 8 Comparison of sodium influx in nsEP and classical electroporation in human Jurkat T Lymphocytes [14]. Cells were exposed to nsEP (30 ns, 25 kV/cm) and Classical EP (30 µs, 5 kV/cm) pulses. No sodium influx was observed in nsEP (**a**) while a spike of sodium ions enters the classical electroporated cells (**b**)

targets. More study in this line would help clarify this mechanism.

Sodium Entry into the cell

Since Ca^{2+} bursts have been shown with nsEP, it is of practical interest to verify if a similar phenomenon applies to sodium also, i.e. diffusion of sodium through the nanopores. For this purpose, sodium green-loaded cells were exposed to both µs and ns pulses of 5 kV/cm, 30 µs and 25 kV/cm, 30 ns, respectively [14]. While electroporation due to conventional µs pulses caused a measurable sodium influx, no noticeable sodium entry was observed for nsEP (Fig. 8) [14].

Nanopulsers

High voltage, ns pulse generators are an integral part of the nsEP research. Due to very short time durations integrated with the high voltages required for these applications, it is very challenging to design and build a successfully functioning ns pulser with minimum oscillations and reflections in the waveform. Advancement in pulsed power technology [16, 17] has enabled the development of a number of nanopulsers using the Blumlein pulse forming network (PFN) concept (Fig. 9) [34]. Various first and second generation nanosecond pulse generators for biological applications were designed and developed primarily by three research groups [11, 12, 28, 31, 34–37]. The various pulsers developed include: 10–300 ns, up to 300 kV/cm, Blumlein pulser; 4 kV, 5 ns, 10 Ω load, inductive adder

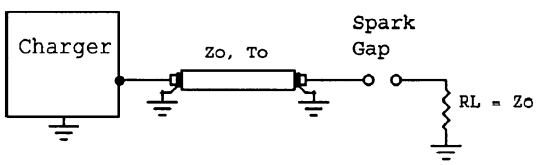

Fig. 9 Pulse forming network (PFN) concept used for nanopulser. Shown here is a single ended transmission PFN with characteristic impedance Zo and transmission delay T_o [34]

charged cable pulser; 10 kV, 5 ns, 20 Ω load, water Blumlein mini-pulse generator; 4 kV, 5 ns, 10 Ω load, ceramic Blumlein mini-pulse generator; 400 V, 5 ns, MOSFET-based micropulser for microscope slide load; 10 kV, 10 ns, 1 kHz, nanosecond flashlamp for real time microscopy of cell electroperturbation; 15 kV, 11 ns, pulser; and 15 kV, 45, 65, and 95 ns pulser. The electric field strength is calculated as $E = V/d$ kV/cm, where V is the voltage in kV and d is the distance in cm between the electrodes. Another simple, but efficient MOSFET-based nanosecond pulse generator was designed and developed at Arizona State University [38]. A simulation study of the influence of various parameters, such as the effect of load on ns rise and fall times, etc. was also performed [39].

60 and 300 ns Pulsers

Two nanopulsers, 60 ns, 60 kV/cm and 10–300 ns, and up to 300 kV/cm were developed by this research group at the Old Dominion University (ODU), using a Blumlein pulse forming network (PFN) [40]. The pulse width of these generators is determined by the length (L) of their transmission lines. A pressurized spark gap was used for fast switching in these pulsers. The 60 kV/cm Blumlein PFN consisted of two 50 Ω coaxial cables to give a total impedance of 100 Ω. The energy stored in the cables is transferred into the matched load in the form of a HV rectangular pulse, whose duration is determined by the cable length and the propagation speed of the electromagnetic waves in the cable dielectric. The load (cuvette with biological cells) must match the source impedance for obtaining the desired waveform. The spark gap that serves as a fast electrical switch has a closing time of <10 ns. This reduces jitter in the wave to less than 5%. With a maximum voltage generation of 2 kV across 1/3 mm electrode gap, this pulser could generate a maximum electric field of (2 kV/(1/3 mm) = 60 kV/cm. The hold-off voltage of the cable connectors will limit this max value to some extent. This nanopulser was connected to the cell chamber containing the cuvette using a microscope slide arrangement to obtain real time imaging. Figure 10 illustrates the

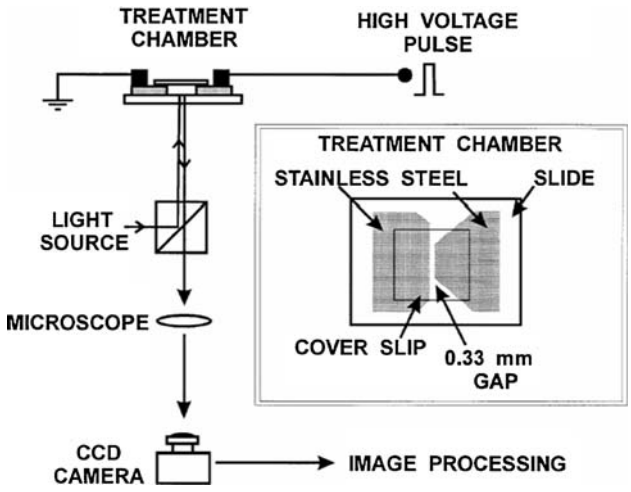

Fig. 10 Experimental set-up of the microscope-based nanopulser system [35, 40]. Cells are placed in between the two stainless steel electrodes and are covered by a cover slip

experimental set-up [35, 40]. An Olympus IX70 inverted microscope was used for this purpose. The chamber comprises a 51 × 76 mm glass microscope slide with two 0.1 mm thick stainless steel electrodes attached to the slide surface with silicone adhesive. The two electrodes were placed 0.33 mm apart to form a 5 mm long channel. Cell suspension (40–70 µl) was placed in this channel. A standard 0.17 mm thick glass slip was used to cover the electrode gap. The channel was aligned with the microscope light path, and solid copper contacts attached to the high-voltage power supply were laid on the stainless steel electrodes.

MOSFET-Based 1 kV Blumlein Pulser

Figure 11 shows the circuit set-up and schematic of another nanosecond pulser, developed by the above group [28]. This also utilizes a Blumlein configuration using high-frequency cables, just as in the above and several of their other pulse generators. A high speed, 1 kV MOSFET was used as a fast switch in this pulser. Using a very narrow electrode gap of 100 µm, this pulser can generate up to 100 kV/cm electric pulses. This very narrow electrode gap was used to study single cells under a microscope (Fig. 11a). The waveform is shown in Fig. 11b. Its rise time is about 3 ns and the length (duration) of the pulse is less than 10 ns. This group built a number of other pulsers with various pulse widths, type of switch, and PFNs, using a similar configuration [28, 41].

MOSFET-based Nanopulser-400 V, 30 ns (Microreactor)

A number of nanopulsers were also developed by this research group at the University of Southern California (USC) [31, 34, 37]. Some of these based on Blumlein configuration, similar to that of the first research group. A MOSFET-based, inductive pulser with a balanced, coaxial-cable pulse-forming network (PFN) and spark gap switch was designed and developed to provide trapezoidal electrical voltage pulses to cell suspensions in growth medium contained in commercial rectangular cuvettes with 1 mm electrode separation [31]. The same system, with a reconfigured PFN, was developed to deliver pulses to a custom exposure chamber built for checking bacteria spores in paper envelopes. In this case, the pulse developed was 150 ns long with fields up to 50 kV/cm with a 7 ns rise time at a frequency of 2 kHz. The electrodes were a copper plate positioned over a copper ground plane. The ground plane was covered by Delrin sheet to reduce corona and prevent arcing at high pulse frequencies.

For microscopic observations, cells were placed in a rectangular channel of 100 µm width, 25 µm depth, and 15 mm length. This was formed by two precision-cut strips of platinum foil attached to a glass microscope slide with paraffin. The platinum strips serve both as electrodes and as the walls of the exposure chamber. The fast RF MOSFET

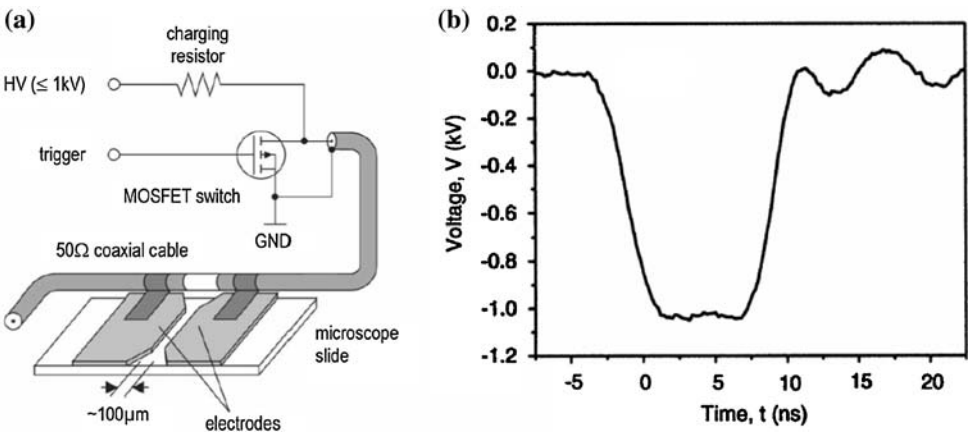

Fig. 11 (**a**) MOSFET + Blumlein-based, 1 kV, nanosecond pulser [28]. With an electrode gap of 100 µm, it is possible to develop electric fields of up to 1 kV/100 µm = 100 kV/cm in this "Microreactor". Cells in suspension are placed between the electrodes. MOSFET is used as a fast switch using Blumlein circuit as shown, (**b**) Nanosecond voltage pulse generated using the above nanopulser

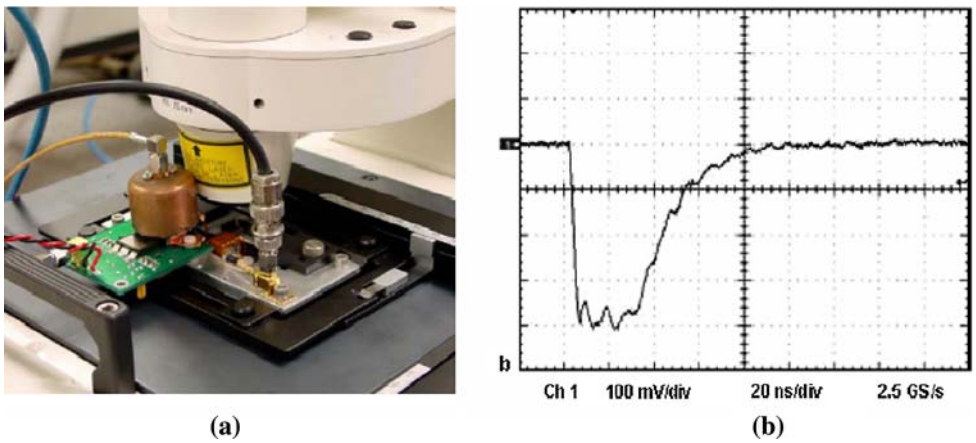

Fig. 12 (**a**) Fast RF MOSFET-based micropulser and microscope slide-based pulse chamber mounted on the stage of a fluorescence microscope, (**b**) micropulser voltage waveform—370 V, 30 ns [31]

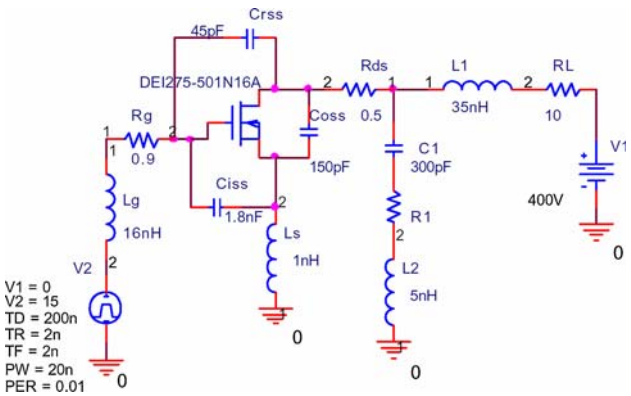

Fig. 13 Charging circuit for the MOSFET-based micropulser delivering nanopulses [37]

Microreactor was mounted on the microscope stage for delivery of pulses directly to the microchamber electrodes (Fig. 12a) [31]. Figure 12b shows the waveform generated. The micropulser RF schematic is shown in Fig. 13 [37]. Details of other pulsers developed by this group can be found in [34, 42].

10–100 Nanosecond Pulse Generators

Two different square wave nanopulsers based on PFN were developed by this group of researchers at ODU, again using PFN [12]. The first pulser was built with a 1 m long strip line as the PFN to generate pulses of a constant length of 11 ± 0.1 ns. Longer pulses were developed using a PFN consisting of several coaxial cables in parallel. The cables varied in length, and hence, the pulse lengths also varied. Thus, using 3, 5, and 9 m cables for the PFN, it was possible to generate 45, 65, and 95 ns pulses respectively. The pulser used a 30 kV Dc power supply for charging; therefore, the load voltage across the matching load will be 50% of the input voltage, 15 kV in this case. A spark-gap operating in the self-breaking mode was used as the fast switch to discharge the stored energy. The matched load was a high-voltage resistor connected in parallel with a 1 mm electrode gap cuvette that holds 100 µl cell suspension. The max electric field that could be generated was 150 kV/cm. The pulse voltage was monitored using a 500 MHz Tektronix digital storage oscilloscope. Figure 14 shows the waveforms obtained in the strip line and parallel cables pulsers [12].

MOSFET-Based 400 V, 75 ns Nanopulser

This MOSFET-based nanopulser was designed to drive a 50 Ω resistive load with 0–400 V, 75 ns pulses at Arizona State University (ASU) [38]. The circuit includes three stages: (1) an integrated variable frequency and variable duration pulsewidth signal source, (2) an inverter/driver stage, and (3) a power buffer consisting of a passively

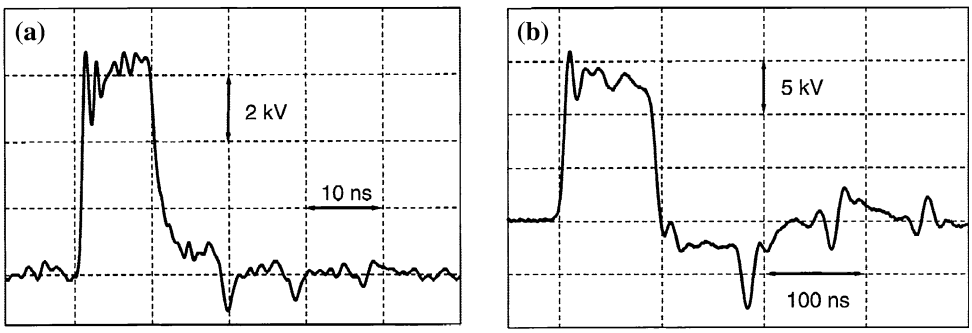

Fig. 14 Nanosecond pulses produced by (**a**) Strip line (10 ns long) and (**b**) parallel cables (95 ns long). PFN using five parallel cables of 9 m long each produced the 95 ns pulse [12]

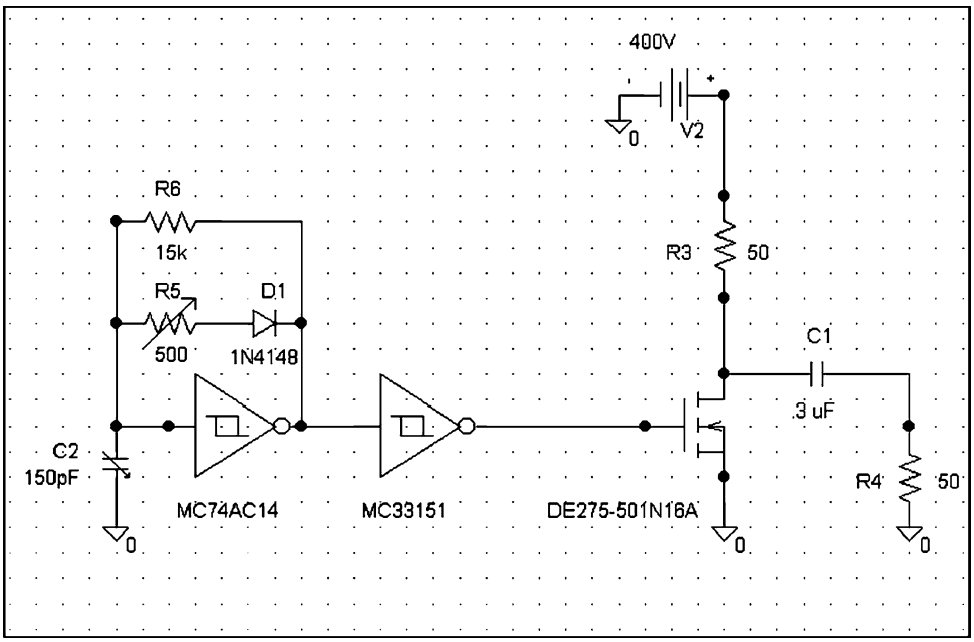

Fig. 15 400 V, 75 ns MOSFET nanopulser circuit schematic—Schmitt trigger produces fast rise time, integrated driver meets the required specifications, and Totel Pole BJT can sink/source 1.5 A to drive fast MOSFET [38]

loaded single power MOSFET. The circuit construction is physically optimized to reduce distortion and retain signal integrity while minimizing reflected power from the circuit and load. The driver used is a MC33151 (On Semiconductor) integrated 15 ns rise time, dual, inverting Schmitt trigger input with totem pole outputs. The buffer is an IXYS DE275-501N16A RF MOSFET with 500 V, 16 A, and with a 6 ns rise time. The MOSFET is biased into cutoff, and the circuit is designed to maximize rise time and operated common source for optimal efficiency. The voltage sources are linear designs with the signal source and driver supplies actively regulated. Since ns pulsers are not available commercially, this circuit was designed and built using components that are mass manufactured for standard consumer applications in a very simple, low cost circuit that will function well as a research quality high-voltage nanopulser for electroporation applications. The circuit (Fig. 15) was implemented using exclusively off-the-shelf devices and was constructed using commercially available RF groundplane microstrip prototype components. Figure 16a shows the construction, and Fig. 16b illustrates the waveform obtained for an input voltage of 400 V. Using 0.1 cm cuvettes, it is possible to generate fields of up to 4 kV/cm magnitude with this pulser.

MOSFET-Based 1000 V, 20 ns Nanopulser

A 0–1000 V, compact (4″ × 4″ × 2″), MOSFET-based nanosecond pulser that operates using a 9.6 V DC rechargeable battery, with variable pulse durations of 20 ns to 20 μs and with variable pulse repetition rate of 1–6 kHz was designed and built at Purdue University [43]. The compact nanopulser could be broken down into three system blocks: (1) high-voltage source block which converts

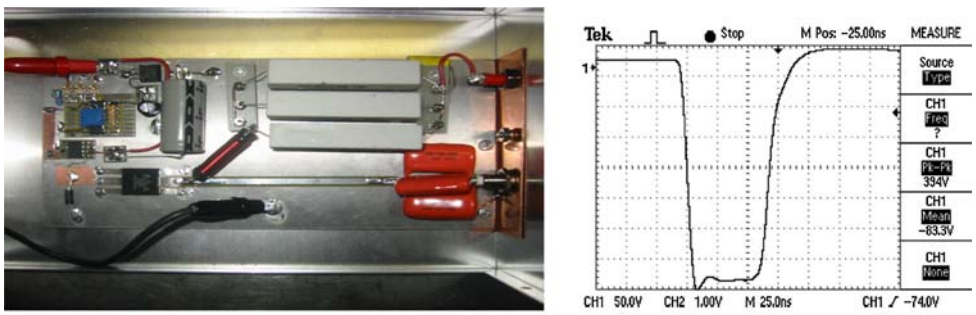

(a) (b)

Fig. 16 (**a**) 400 V, 75 ns nanopulser-prototype with ground plane and solder mount on surfboard PCB-transmission line construction, (**b**) Output voltage pulse waveform with 50 Ω load-input voltage applied was 408 V and output voltage obtained was 394 V. Horizontal scale is 25 ns/div and the vertical scale is 50 V/div. The pulse width is 70 ns. The fall time is about 10 ns. The waveform was recoded using a Tektronix.TDS 210, 60 MHz, 1GS/s Digital Storage Scope [38]

the battery's 9.6 V DC to a variable high-voltage output and stores this charge for use when the pulsing begins, (2) the switching block, which is a MOSFET-based low-side switch that applies short nanosecond pulses to the load, and (3) the pulse generation block that generates a short nanosecond pulse and supplies enough current to adequately turn the MOSFET on fast enough to apply a nanosecond pulse to the load.

Since the goal of this project was to keep the pulser as small as possible and portable, high-voltage DC–DC converters were used. These high-voltage modules convert 0–12 V DC to 0–1,500 V DC. A potentiometer is used to achieve the desired output voltage. Two diodes were used on the output of the high-voltage module to protect it from transient spikes and damage. The module charges a 1 μF capacitor, which is used to provide energy to the load when pulsed.

The nanosecond pulse generator circuit was constructed using two CMOS digital ICs based on a published report [44]. One IC was a retriggerable monostable multivibrator and the other was a D flip flop. A potentiometer is added in series with the external resistor allowing for adjustment to the pulse duration. These pulses are then used to clock and preset the D flip flop. The retriggerable monostable multivibrator needs a clock signal to repeat pulses. A simple 555 timer was used to create a CMOS clock of 1.5 kHz. The 555 timer is also built with potentiometers to vary frequency and duty cycle. All three ICs were powered using a simple 5 V DC regulator. To achieve pulse durations as low as 20 ns, an extremely fast RF MOSFET (IXZR08N120B RF Power MOSFET) by IXYS was chosen as the switch. It is rated at 1200 V. A high-current driver was used to switch the MOSFET by charging the MOSFET gate capacitance of 1,960 pF. The driver also has to be very fast, so a 4 ns rise time MOSFET driver (DEIS420) was chosen. The pulser was built using PCB layouts (Fig. 17). The top copper of the PCB contains the majority of the components and trace routes. Most of the nanosecond switching and pulse generation blocks are laid out on the top layer. The bottom copper of the PCB was used for the power supplies, high-voltage source block, and ground plane. Placement of components was closely watched to reduce critical route lengths and crosstalk. Figure 18a shows the construction, and Fig. 18b illustrates the 1000 V waveform generated using this pusler.

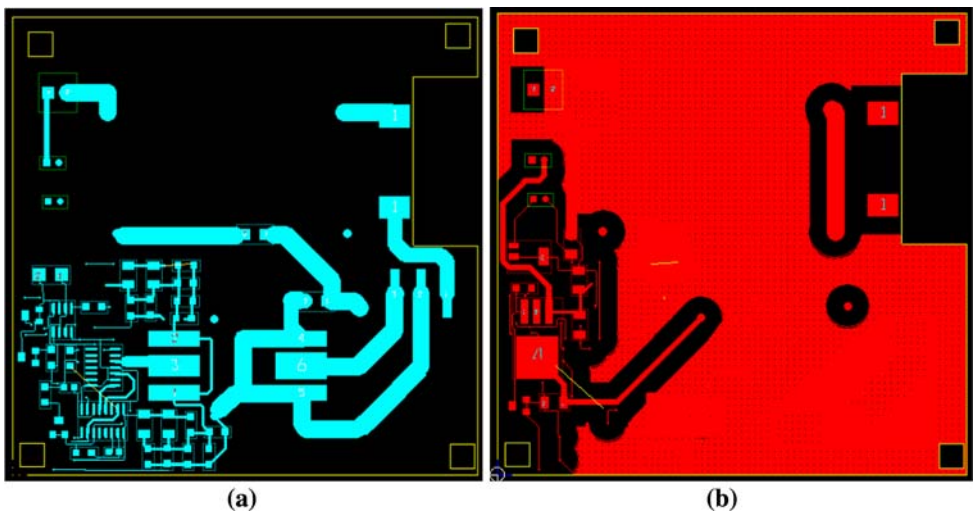

Fig. 17 PCB top (**a**) and bottom (**b**) copper layouts [43]

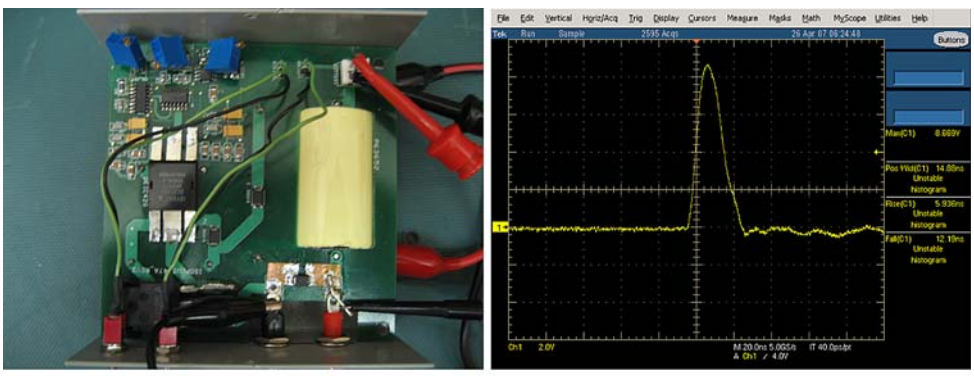

Fig. 18 (**a**) 1000 V, 20 ns nanopulser, (**b**) 1000 V output voltage pulse waveform. Horizontal scale is 20 ns/div and the vertical scale is 1 V/div. The pulse width is about 20 ns. The waveform was recoded using a Tektronix TDS 5032B, 300 MHz, 5MS/s Digital Storage Scope and a 100× probe [43]

Discussion and Conclusion

The prediction that electric fields of appropriate magnitudes at high frequencies should be capable of coupling electrical energy into the interior, and therefore, into the internal organelles of biological cells was made by Schwan [45]. However, it is only in the last few years with the advancements in the pulsed power technology that sufficiently short and intense pulses of electric field have been applied to cells to evoke the interesting and potentially very useful effects that are possible by selective manipulation of such intra-cellular compartments. The latest technological advances have enabled today's researchers to design and develop ns pulse generators that can operate at high voltages. Nanosecond (10–300 ns), high-intensity (10–300 kV/cm) electric pulses have shown to induce increases in the intracellular concentration of cytosolic calcium and the translocation of phosphatidylserine to the outer layer of the plasma membrane in human Jurkat T lymphoblasts as observed by various researchers. PS externalization in living cells exposed to nanosecond, several kV/cm electric pulses indicate the development of nanometer-diameter aqueous pores within nanoseconds after application of high-intensity nanopulses, and electrophoretic transport of the anionic PS headgroup along the newly constructed hydrophilic pore surface commences even while pore formation is still in progress [46]. PS exposure plays an important role in normal tissues, marking cells for phagocytosis and removal. Once the basis of this mechanism is understood, activating PS using nanosecond pulses would offer intriguing possibilities for fundamental biophysical investigations and for treatment of diseases. In addition, nsEP also illustrated that low-conductivity media (whose conductivity is lower than that of the cytosol) can greatly improve the electropermeabilization via the electrical stretching force exerted on the cell membrane as in classical electroporation [12].

Nanopulse-induced calcium bursts occurred within milliseconds and PS externalization occurred within minutes of the pulse exposure. Caspase activation and other indicators of apoptosis followed these initial apoptotic signals. Pulse-induced PS translocation was observed even in the presence of caspase inhibitors. Similar observations were also made using ultra-sound pulses [25, 26, 47]. Using low-intensity ultra-sound pulses [25], they observed apoptosis, PS translocation, and other effects observed similar to nsEP. The high-intensity nanopulse electroporation effects differ markedly from classical electroporation effects. The electroperturbations produced by the nanopulses are due to the intracellular disturbances of physiological equilibria, while the integrity of the external plasma membrane is maintained. Thus, nsEP offers new ways to manipulate the contents of living cells.

The results reviewed here clearly demonstrate that nanosecond pulses of high magnitudes can be used for injecting membrane impermeable molecules into mammalian cells without significantly affecting the external plasma membrane. Nanosecond, high-intensity pulses (with low energy) extend the reach of an external electric field to the nuclear and mitochondrial membranes, to the nucleoplasm and the mitochondrial matrix, and to the membranes and contents of storage vacuoles and other intracellular compartments. Manipulation of these compartments can trigger apoptosis and other cell controlling signals. Thus, nsEP also has the potential for selective electromanipulation of intracellular membrane-bound organelles and for targeting malignant cells in a mixed population of cancerous and healthy cells [12, 13, 28, 35]. With appropriate pulse generators, it is possible to perform in situ electropermeabilization of organelles within the cell without deteriorating the plasma membrane. This technique could be used for the manipulation of the mitochondrial genome, which is essential for the analysis of molecular pathology and for therapy of a large group of mitochondrial disorders [12].

Acknowledgments The author is very grateful to her students, Jim Gonzales, Jin Shao, Alton Chaney, Esaki Soundarajan (at Arizona State University East), and Jason Harper and Drew Cambell (at Purdue University) for their major contributions in designing and building the pulsers and to Josh Hutcheson, School of Chemical and Biomolecular Engineering of Georgia Institute of Technology for his excellent editing of the manuscript.

References

1. Heller, R., Jaroszeski, M., Grass, L., Messina, J., Rapaport, D., Deconti, R., et al. (1996). Phase I/II trial for the treatment of cutaneous and subcutaneous tumors using electrochemotherapy. *Cancer, 77*, 964–971. doi:10.1002/(SICI)1097-0142(19960301)77:5<964::AID-CNCR24>3.0.CO;2-0.
2. Gehl, J., & Geertsen, P. F. (2000). Efficient palliation of haemorrhaging malignant melanoma skin metastases by electrochemotherapy. *Melanoma Research, 10*, 1–5. doi:10.1097/00008390-200012000-00011.
3. Mir, L. M., et al. (1999). High efficiency gene transfer into skeletal muscle mediated by electric pulses. *Proceedings of the National Academy of Sciences of the United States of America, 96*, 4262–4267. doi:10.1073/pnas.96.8.4262.
4. Dev, S. B., Rabussay, D. P., Widera, G., & Hofmann, G. A. (2000). Medical applications of electroporation. *IEEE Transactions on Plasma Science, 28*, 206–223. doi:10.1109/27.842905.
5. Heller, R., Gilbert, R., & Jaroszeski, M. J. (2000). Clinical trials for solid tumors using electrochemotherapy. In M. Jaroszeski, R. Heller & R. Gilbert (Eds.), *Electrochemotherapy, electrogenetherapy, and transdermal delivery* (pp. 137–156). New Jersey: Humana Press.
6. Gothelf, A., Mir, L., & Gehl, J. (2003). Electrochemotherapy: Results of cancer treatment using enhanced delivery of bleomycin by electroporation. *Cancer Treatment Reviews, 29*, 371–387. doi:10.1016/S0305-7372(03)00073-2.

7. Rodriguez-Cuevas, S., Barroso-Bravo, S., Almanza-Estrada, J., Cristobal-Marinez, L., & Gonzalez-Rodriguez, E. (2001). Electrochemotherapy in primary and metastatic skin tumors: Phase II Trial using intralesional bleomycin. *Archives of Medical Research, 32*, 273–276. doi:10.1016/S0188-4409(01)00278-8.
8. Jaroszeski, M., Gilbert, R., Nicolau, C., & Heller, R. (2000). Delivery of genes in vivo using pulsed electric fields. In M. Jaroszeski, R. Heller & R. Gilbert (Eds.), *Electrochemotherapy, electrogenetherapy, and transdermal delivery* (pp. 173–186). New Jersey: Humana Press.
9. Martin, J. B., Young, J. L., Benoit, J. N., & Dean, D. A. (2000). Gene transfer to intact mesenteric arteries by electroporation. *Journal of Vascular Research, 37*, 372–380. doi:10.1159/000025753.
10. Schoenbach, K. H., Beebe, S. J., & Buescher, E. S. (2001). Intracellular effect of ultrashort electrical pulses. *Bioelectromagnetics, 22*, 440–448. doi:10.1002/bem.71.
11. Beebee, S. J., Fox, P. M., Rec, L. J., Willis, E. L., & Schoenbach, K. H. (2003). Nanosecond, high-intensity pulsed electric fields induce apoptosis in human cells. *The FASEB Journal, 17*, 1493–1495.
12. Muller, K. J., Sukhorukov, V. L., & Zimmermann, U. (2001). Reversible electropermeabilization of mammalian cells by high-intensity, ultra-short, pulses of submicrosecond duration. *The Journal of Membrane Biology, 184*, 161–170. doi:10.1007/s00232-001-0084-3.
13. Vernier, P. T., Li, A., Marcu, L., Craft, C. M., & Gundersen, M. A. (2003). Ultrashort pulsed electric fields induce membrane phospholipids translocation and caspase activation: Differential sensitivities of Jurkat T lymphoblasts and rat glioma C6 cells. *IEEE Transactions on Dielectrics and Electrical Insulation, 10*, 795–809. doi:10.1109/TDEI.2003.1237329.
14. Vernier, P. T., Sun, Y., Marcu, L., Salemi, S., Craft, C., & Gundersen, M. A. (2003). Calcium bursts induced by nanosecond electric pulses. *Biochemical and Biophysical Research Communications, 310*, 286–295. doi:10.1016/j.bbrc.2003.08.140.
15. Schwan, H. P. (1989). Dielectrophoresis and rotation of cells. In E. Neumann, A. E. Sowers & C. A. Jordan (Eds.), *Electroporation and electrofusion in cell biology* (pp. 3–21). New York: Plenum Press.
16. Kristiansen, M., & Hagler, M. O. (1987). Pulsed power systems. In R. A. Meyers (Ed.), *Encyclopedia of physical science and technology* (Vol. 11, pp. 410–419). Orlando: Academic Press.
17. Schoenbach, K. H., Peterkin, F. E., Alden, W. A., & Beebee, S. J. (1997). The effect of pulsed electric fields on biological cells: Experiments and applications. *IEEE Transactions on Plasma Science, 25*, 284–292. doi:10.1109/27.602501.
18. Mussauer, H., Sukhorukov, V. L., Haase, A., & Zimmermann, U. (1999). Resistivity of red blood cells against high intensity, short-duration electric field pulses induced by chelating agents. *The Journal of Membrane Biology, 170*, 121–133. doi:10.1007/s002329900542.
19. Schoenbach, K. H., Katsuki, S., Stark, R. H., Buescher, E. S., & Beebe, S. J. (2002). Bioelectrics—new applications for pulsed power technology. *IEEE Transactions on Plasma Science, 30*, 293–300. doi:10.1109/TPS.2002.1003873.
20. Ellappan, P., & Sundararajan, R. (2005). A simulation study of the electrical model of biological cells. *Journal of Electrostatics, 63*, 297–307. doi:10.1016/j.elstat.2004.11.007.
21. Schwan, H. P. (1989). Dielectric properties of tissues and biological materials: A critical review. *Critical Reviews in Biomedical Engineering, 17*, 25–104.
22. Beebe, S. J., Blackmore, P. F., White, J., Joshi, R. P., & Schoenbach, K. H. (2004). Nanosecond pulsed electric fields modulate cell function through intracellular signal transduction mechanisms. *Physiological Measurement, 25*, 1077–1093. doi:10.1088/0967-3334/25/4/023.
23. Mastrangelo, A. J., Hardwick, J. M., & Betenbaugh, M. J. (2000). Overexpression of bcl-2 family members enhances survival of mammalian cells in response to various culture insults. *Biotechnology and Bioengineering, 67*, 555–564. doi:10.1002/(SICI)1097-0290(20000305)67:5<555::AID-BIT6>3.0.CO;2-T.
24. Hofmann, F., Ohnimus, H., Scheller, C., Strupp, W., Zimmermann, U., & Jassoy, C. (1999). Electric field pulses can induce apoptosis. *The Journal of Membrane Biology, 169*, 103–109. doi:10.1007/s002329900522.
25. Ashush, H., Rozenszajn, L. A., Blass, M., Barda-Saad, M., Azimov, D., Radnay, J., et al. (2000). Apoptosis induction of human myeloid leukemic cells by ultrasound exposure. *Cancer Research, 60*, 1014–1020.
26. Feril, L. B., & Kondo, T. (2004). Biological effects of low intensity ultrasound: The mechanism involved, and its implications on therapy and biosafety of ultrasound. *Journal of Radiation Research, 45*, 479–489. doi:10.1269/jrr.45.479.
27. Kroemer, G., Dallaporta, B., & Resche-Rigon, M. (1998). The mitochondrial death/life regulator in apoptosis and necrosis. *Annual Review of Physiology, 60*, 619–642. doi:10.1146/annurev.physiol.60.1.619.
28. Schoenbach, K. H., Joshi, R. P., Kolb, J. F., Nianyong, C., Stacey, M., Blackmore, P. F., et al. (2004). Ultrashort electrical pulses open a new gateway into biological cells. *Proceedings of the IEEE, 92*, 1122–1137. doi:10.1109/JPROC.2004.829009.
29. Tyurina, Y. Y., Serinkan, F. B., Tyurint, V. A., Kini, V., Yalowich, J. C., Schroit, A. J., et al. (2004). Lipid antioxidant, etoposide, inhibits phosphatidylserine externalization and macrophage clearance of apoptotic cells by preventing phosphatidylserine oxidation. *The Journal of Biological Chemistry, 279*, 6056–6064. doi:10.1074/jbc.M309929200.
30. Naito, M., Nagashima, K., Mashima, T., & Tsuruo, T. (1997). Phosphatidylserine externalization is a downstream event of interleukin-1b-converting enzyme family protease activation during apoptosis. *Blood, 89*, 2060–2066.
31. Vernier, P. T., Sun, Y., Marcu, L., Carft, C. M., & Gundersen, M. A. (2004). Nanoelectropulse-induced phosphatidylserine translocation. *Biophysical Journal, 86*, 4040–4048. doi:10.1529/biophysj.103.037945.
32. Hall, E. H., Schoenbach, K. H., & Beebe, S. J. (2005). Nanosecond pulsed electric fields (nsPEF) induce direct electric field effects and biological effects on human colon carcinoma cells. *DNA and Cell Biology, 24*, 283–291. doi:10.1089/dna.2005.24.283.
33. Beebe, S. J., Fox, P. M., Rec, L. J., Somers, K., Stark, R. H., & Schoenbach, K. H. (2002). Nanosecond pulsed electric field (nsPEF) effects on cells and tissues: Apoptosis induction and tumor growth inhibition. *IEEE Transactions on Plasma Science, 30*, 286–292. doi:10.1109/TPS.2002.1003872.
34. Behrend, M., Kuthi, A., Xianyue, G., Vernier, P. T., Marcu, L., Craft, C. M., et al. (2003). Pulse generators for pulsed electric field exposure of biological cells and tissues. *IEEE Transactions on Dielectrics and Electrical Insulation, 10*, 820–825. doi:10.1109/TDEI.2003.1237331.
35. Buescher, E. S., & Schoenbach, K. H. (2003). Effects of submicrosecond, high intensity, pulsed electric fields on living cells-intracellular electromanipulation. *IEEE Transactions on Dielectrics and Electrical Insulation, 10*, 788–795. doi:10.1109/TDEI.2003.1237328.
36. Vernier, P. T., Thu, M. M. S., Marcu, L., Craft, C. M., & Gundersen, G. A. (2004). Nanosecond electroperturbation-mammalian cell sensitivity and bacterial spore resistance. *IEEE Transactions on Plasma Science, 32*, 1620–1625. doi:10.1109/TPS.2004.831754.
37. Behrend, M., Kuthi, A., & Vernier, P. T. (2002). Micropulser for real-time microscopy of cell electroperturbation In: International Power Modulator Conference, Hollywood, CA, pp. 358–361.

38. Chaney, A., & Sundararajan, R. (2004). Simple MOSFET-based high voltage nanosecond pulse circuit. *IEEE Transactions on Plasma Science, 32*, 1919–1924. doi:10.1109/TPS.2004.835966.
39. Sundararajan, R., Shao, J., Soundararajan, E., Gonzales, J., & Chaney, A. (2004). Performance of solid state high voltage pulsers for biological applications—a preliminary study. *IEEE Transactions on Plasma Science, 32*, 2017–2025. doi:10.1109/TPS.2004.835944.
40. Hair, P. S., Schoenbach, K. H., & Buescher, E. S. (2003). Submicrosecond, intense pulsed electric field applications to cells show specificity effects. *Bioelectroschemsitry, 61*, 65–72. doi:10.1016/S1567-5394(03)00076-8.
41. Deng, J., Schoenbach, K. H., Buescger, E. S., Hair, P. S., Fox, P. M., & Beebe, S. J. (2003). The effects of intense submicrosecond electrical pulses on cells. *Biophysical Journal, 84*, 2709–2714.
42. Yinghua, S., Vernier, P. T., Behrend, M., Marcu, L., & Gundersen, M. A. (2005). Electrode microchamber for noninvasive perturbation of mammalian cells with nanosecond pulsed electric fields. *IEEE Transactions on Nanobioscience, 4*(5), 277–283.
43. Campbell D., Harper J. (2007) Miniature high voltage MOSFET based nanosecond pulser. *Final project Report*, ECET 581A course, Spring, Purdue University.
44. http://www.edn.com/article/CA46850.html), April 2007.
45. Schwan, H. P. (1985). Dielectric properties of cells and tissues. In A. Chiabrera, C. Nicolini & H. P. Schwan (Eds.), *Interactions between electromagnetic fields, and cells* (pp. 75–97). New York: Pergamon.
46. Feril, L. B., Kondo, T., Takaya, K., & Riesz, P. (2004). Enhanced ultrasound-induced apoptosis and cell lysis by a hypotonic medium. *International Journal of Radiation Biology, 80*, 165–175. doi:10.1080/09553000310001654684.
47. Vernier, P. T., Ziegler, M. J., Sun, Y., Chang, W. V., Gundersen, M. A., & Tieleman, D. P. (2006). Nanopore formation and phosphatidylserine externalization in a phospholipids bilayer at high transmembrane potential. *Journal of the American Chemical Society, 128*, 6288–6289. doi:10.1021/ja0588306.